Contribution from the Department of Chemistry,
University of Kentucky, Lexington, Kentucky 40506

Electronic Spectra of Pseudotetrahedral (C_{2v}) Complexes. Cobalt(II) Compounds

E. ROLAND MENZEL, WILLIAM R. VINCENT, DIANA K. JOHNSON, GERALD L. SEEBACH, and JOHN R. WASSON*

Received February 15, 1974 AIC40105P

A novel variation of the weak ligand field treatment of the electronic spectra of transition metal complexes of the type MA_2B_2 with C_{2v} symmetry is presented and tested with data for various pseudotetrahedral cobalt(II) compounds. A marked improvement in fit of theory to experiment is found over previous models. The explicit account taken of some covalency effects without incurring additional complexity of the model may alleviate some of the conceptual shortcomings inherent in the electrostatic point-charge approximation to metal–ligand interactions while retaining its attractive simplicity.

Introduction

The extensive growth of transition metal chemistry has necessitated the development of models to account for and predict the electronic spectra and magnetic properties of complexes possessing lower than cubic symmetry. Compounds possessing metal ions with d^1,^{9} electronic configurations have been examined[1-3] but complexes with other d^n configurations have received less attention. The electronic spectra of high-spin cobalt(II) $3d^7$ complexes of the types CoX_4, CoA_3B, and CoA_2B_2 (X, A, B = monodentate ligands) of tetrahedral, pseudotetrahedral C_{3v}, and pseudotetrahedral C_{2v} symmetry, respectively, have been studied extensively.[4-13] The observed "d ← d" bands occur at roughly 3, 6, and 15 kK (1 kK = 1000 cm^{-1}). The two lower energy absorptions correspond to orbital triplets of the ^4F term (in tetrahedral symmetry) while the highest one arises from the ^4P free ion term and is also triply degenerate in tetrahedral symmetry. These degeneracies are lifted partially on going to C_{3v} and completely in C_{2v} pseudotetrahedral complexes. Ligand field calculations within the weak-field approximation yield a reasonable correlation between calculated and observed centers of gravity of the orbital triplets[5] but calcualted splittings in the pseudotetrahedral cases often agree poorly with experiment.[14] These discrepancies between theory and experiment have been attributed to lack of consideration of (i) spin–orbit coupling, (ii) vibronic coupling, (iii) mixing of ^2G and ^4P states, and (iv) Jahn–Teller distortions. Mechanisms (i) and (iii) are listed separately even though (iii) arises from spin–orbit coupling, too, in order explicity to account for spin–orbit effects within a given ^{2S+1}L manifold. However, the difficulties with the electrostatic point-charge model inherent in the weak ligand field approach extend even further—covalency effects are not explicitly accounted for. Purely electrostatic considerations are not capable of unified interpretation of parameter trends in terms of the nephelauxetic and spectrochemical series. Although molecular orbital theory provides a conceptually more satisfying approach to the description of metal–ligand interactions, the semiempirical MO methods usually employed often lead to predictions of questionable reliability because of gross approximations required to keep computations sufficiently simple to remain tractable. The weak ligand field model thus remains very attractive because of its intrinsic simplicity and in many cases because of its quantitative usefulness in interpretation of observed spectra as long as parameters are treated purely empirically. If covalency effects can be accounted for in order to yield additional physical insight without increase in computational complexity, the utility of the weak-field model would be enhanced, particularly, if attendant improvement in fit to experiment results.

Herein we report the electronic spectra of $Co(apy)_2X_2$ (apy = antipyrine (1-phenyl-2,3-dimethyl-5-pyrazolone); X^- = Cl^-, Br^-, I^-, and NCS^-) complexes and reexamine the usual ligand field model[14] in hope of deriving an alternate but equally straightforward formulation, which might interpret experimental results with improved precision and yield insight into covalency effects.

Experimental Section

The preparation and spectral and magnetic properties of the cobalt(II)–antipyrine compounds considered here will be reported elsewhere.[15] Room-temperature electronic spectra (Figures 1 and 2) of the complexes in dichloromethane solution were recorded with a Cary Model 14 spectrometer. Gaussian analyses of the electronic spectra were performed using the program BIGAUSS.[16] Calculations were performed using an IBM 360-65 digital computer at the University of Kentucky Computer Center.

Ligand Field Treatment

Initially we consider the mechanisms which, when neglected, form the rationale for inadequacy of fit of the customary weak-field model to experiment.[14] In C_{2v} symmetry, orbital degeneracies are completely lifted and Jahn–Teller splittings need not be considered. With regard to the possible excess number of observed absorption peaks in a "parent tetrahedral" band, vibronic coupling alone is ineffective since the spin-multiplicity selection rule holds.[17] Additional structure can arise only *via* spin–orbit coupling induced admixture of spin-quartet character to spin-doublet states

(1) D. W. Smith, *Struct. Bonding (Berlin)*, 12, 49 (1972).
(2) A. L. Companion and M. A. Komarynsky, *J. Chem. Educ.*, 41, 257 (1964); J. R. Wasson and H. J. Stoklosa, *ibid.*, 50, 186 (1973).
(3) H. J. Stoklosa and J. R. Wasson, *J. Inorg. Nucl. Chem.*, 36, 227 (1973); D. K. Johnson, H. J. Stoklosa, J. R. Wasson, and H. E. Montgomery, *ibid.*, in press.
(4) B. R. Judd, *Proc. Phys. Soc., London*, 84, 1036 (1964).
(5) J. E. Ferguson, *J. Chem. Phys.*, 32, 528 (1960); 39, 116 (1963).
(6) R. L. Carlin and S. L. Holt, Jr., *Inorg. Chem.*, 2, 849 (1963).
(7) A. B. P. Lever and S. M. Nelson, *J. Chem. Soc. A*, 859 (1966).
(8) F. A. Cotton, D. M. L. Goodgame, and M. Goodgame, *J. Amer. Chem. Soc.*, 83, 4690 (1961).
(9) C. Simo and S. L. Holt, *Inorg. Chem.*, 7, 2655 (1968).
(10) M. Goodgame and F. A. Cotton, *J. Amer. Chem. Soc.*, 84, 1543 (1962).
(11) D. M. Gruen and C. A. Angell, *Inorg. Nucl. Chem. Lett.*, 2, 75 (1966).
(12) B. D. Bird and P. Day, *J. Chem. Phys.*, 49, 392 (1968).
(13) M. B. Quinn and D. W. Smith, *J. Chem. Soc. A*, 2496 (1971).
(14) A. Flamini, L. Sestili, and C. Furlani, *Inorg. Chim. Acta*, 5, 241 (1971).
(15) J. Gopalakrishnan and C. C. Patel, *Indian J. Chem.*, 5, 364 (1967); D. K. Johnson, G. L. Seebach, E. R. Menzel, J. R. Wasson, and D. L. Greene, to be submitted for publication.
(16) P. E. Rakita, S. J. Kopperl, and J. P. Fackler, Jr., *J. Inorg. Nucl. Chem.*, 30, 2139 (1968).
(17) S. P. McGlynn, T. Asumi, and M. Kinoshita, "Molecular Spectroscopy of the Triplet State," Prentice-Hall, Englewood Cliffs, N. J., 1969.

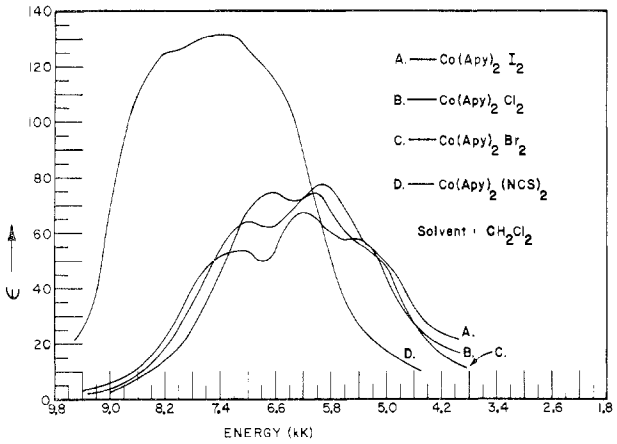

Figure 1. Near-infrared spectra of $Co(apy)_2X_2$ complexes (dichloromethane solutions at room temperature).

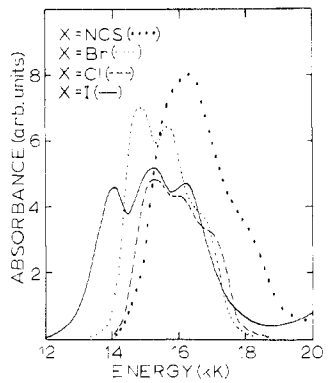

Figure 2. Visible spectra of $Co(apy)_2X_2$ complexes (dichloromethane solutions at room temperature).

which lie near the ^4P term, particularly the ^2G manifold. In general, the various mechanisms responsible for the structure of the "d ← d" electronic spectra of transition metal ions appropriate to the weak-field case are expected to be in the following decreasing order of magnitude: (i) free-ion splitting, (ii) ligand field splitting, (iii) spin-orbit coupling, and (iv) Jahn-Teller distortion, vibronic coupling, etc. A reasonably adequate interpretation of d ← d electronic transitions might be expected to result from simultaneous diagonalization of the Hamiltonian matrices of (i) and (ii) with subsequent addition of (iii) by perturbation methods while (iv) is neglected. In transition metals of relatively low atomic number, such as cobalt, spin-orbit coupling is expected to be small compared to ligand field splitting. Omitting consideration of (iii) should still yield reasonable agreement between calculation and experiment. Somewhat surprisingly, ligand field calculations for pseudotetrahedral complexes of the types of interest here have not shown satisfactory correspondence to observed spectral details. We therefore reexamine the physical assumptions underlying the formulation of the ligand field Hamiltonian, keeping in mind the desirability of inclusion of covalency considerations without incurring additional complexity.

The basic approach to ligand field calculations customarily treats the ligands as effective point charges, $^iE_{eff}$, located at distances, R_i, from the origin of coordinates at which the metal ion is situated. The electrostatic Hamiltonian then describes the interaction between the valence electrons of the central metal ion with the point-charge ligands. In the prevailing model, as described, for instance, by Flamini, Sestili, and Furlani,[14] each ligand is assigned the same effective charge and the distances R_i are essentially treated as empirical parameters. One value of R_i is chosen for each kind of ligand. In the model discussed below, and applied to $Co(apy)_2X_2$ complexes, tetrahedral angles and distances are maintained and the effective charges of the ligands are varied instead. R_i, now the same for the four ligands, is also parameterized; The physical difference between the two approaches is diagrammed in Figure 3. The above-mentioned mechanisms (iii) and (iv) are neglected. Matrix elements were calculated using basis states[18] listed in Table I. The procedure employed to obtain matrix elements is well documented.[19] The energy matrix shown in Table II is obtained. As usual, the Racah parameter, B, gives the free-ion splitting, $15B$, between the ^4F and ^4P terms. Spin-doublet states are not of concern since they were not observed experimentally and do not interact significantly with the quar-

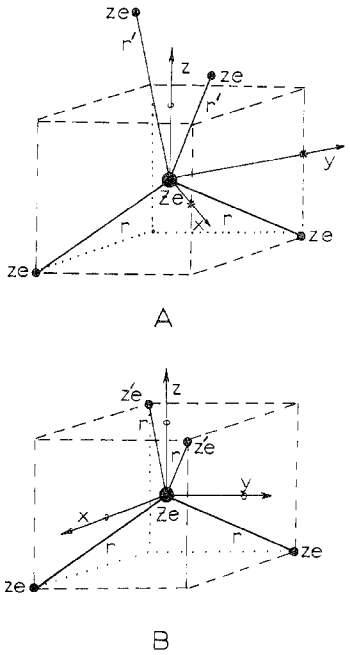

Figure 3. Schematic representation of the physical situation underlying (A) the customary weak-field method and (B) the model employed in this paper. Small circles indicate the intersections of axes with cube faces; asterisks indicate the intersections of axes with cube edges.

Table I. Basis Functions of the Quartet States for the d^3 (or d^7) Electronic Configuration[a]

^{2S+1}L	$\|L, M_L\rangle$	$\sum_i C_i \|\prod_{j=1}^{3} m_{l_j}^{+}\rangle^b$
^4F	$\|3, 3\rangle$	$\|2^+, 1^+, 0^+\rangle$
	$\|3, 2\rangle$	$\|2^+, 1^+, -1^+\rangle$
	$\|3, 1\rangle$	$\sqrt{2/5}\,\|2^+, 1^+, -2^+\rangle + \sqrt{3/5}\,\|2^+, 0^+, -1^+\rangle$
	$\|3, 0\rangle$	$\sqrt{4/5}\,\|2^+, 0^+, -2^+\rangle + \sqrt{1/5}\,\|1^+, 0^+, -1^+\rangle$
	$\|3, -1\rangle$	$\sqrt{2/5}\,\|2^+, -1^+, -2^+\rangle + \sqrt{3/5}\,\|1^+, 0^+, -2^+\rangle$
	$\|3, -2\rangle$	$\|1^+, -1^+, -2^+\rangle$
	$\|3, -3\rangle$	$\|0^+, -1^+, -2^+\rangle$
^4P	$\|1,1\rangle$	$-\sqrt{3/5}\,\|2^+, 1^+, -2^+\rangle + \sqrt{2/5}\,\|2^+, 0^+, -1^+\rangle$
	$\|1, 0\rangle$	$-\sqrt{1/5}\,\|2^+, 0^+, -2^+\rangle + \sqrt{4/5}\,\|1^+, 0^+, -1^+\rangle$
	$\|1, -1\rangle$	$-\sqrt{3/5}\,\|2^+, -1^+, -2^+\rangle + \sqrt{2/5}\,\|1^+, 0^+, -2^+\rangle$

[a] Reference 18. [b] The quantum number $m_{s_j} = +1/2$ appears as a superscript + on the quantum number m_{l_j}.

(18) H. L. Schlafer and G. Gliemann, "Basic Principles of Ligand Field Theory," Wiley, New York, N. Y., 1969, p 242.

(19) M. T. Hutchings, *Solid State Phys.*, 16, 227 (1964); ref 18, Part B; H. Watanabe, "Operator Methods in Ligand Field Theory," Prentice-Hall, Englewood Cliffs, N. J., 1966, Chapter 4.

Table II. Matrix Elements of the Free-Ion and Ligand Field Interactions for Spin-Quartet States and the d^7 Electronic Configuration[a]

|3, 3)	|3, 2)	i|3, 1)	i|3, 0–	|3, −1)	|3, −2)	i|3, −3)	i|1, 1)	i|1, 0)	|1, −1)
$-15B - \frac{6}{27}A_4$		$\frac{24\sqrt{15}}{7\times 27}\bar{A}_4 + \frac{4\sqrt{15}}{7\times 15}\bar{A}_2$		$\frac{-2\sqrt{15}}{27}A_4$			$\frac{4\sqrt{10}}{7\times 27}\bar{A}_4 + \frac{24\sqrt{10}}{7\times 15}\bar{A}_2$		$\frac{-2\sqrt{10}}{27}A_4$
	$-15B + \frac{14}{27}A_4$		$\frac{-4\sqrt{30}}{7\times 27}\bar{A}_4 + \frac{4\sqrt{30}}{7\times 15}\bar{A}_2$		$\frac{-10}{27}A_4$			$\frac{-8\sqrt{30}}{7\times 27}\bar{A}_4 + \frac{8\sqrt{30}}{7\times 15}\bar{A}_2$	
		$-15B - \frac{2}{27}A_4$		$\frac{80}{7\times 27}\bar{A}_4 - \frac{24}{7\times 15}\bar{A}_2$		$\frac{-2\sqrt{15}}{27}A_4$	$\frac{-2\sqrt{6}}{27}A_4$		$\frac{-20\sqrt{6}}{7\times 27}\bar{A}_4 - \frac{8\sqrt{6}}{7\times 15}\bar{A}_2$
			$-15B - \frac{12}{27}A_4$		$\frac{4\sqrt{30}}{7\times 27}\bar{A}_4 - \frac{4\sqrt{30}}{7\times 15}\bar{A}_2$			$\frac{8}{27}A_4$	
				$-15B - \frac{2}{27}A_4$		$\frac{24\sqrt{15}}{7\times 27}\bar{A}_4 + \frac{4\sqrt{15}}{7\times 15}\bar{A}_2$	$\frac{-20\sqrt{6}}{7\times 27}\bar{A}_4 - \frac{8\sqrt{6}}{7\times 15}\bar{A}_2$		$\frac{-2\sqrt{6}}{27}A_4$
					$-15B + \frac{14}{27}A_4$			$\frac{-8\sqrt{30}}{7\times 27}\bar{A}_4 + \frac{8\sqrt{30}}{7\times 15}\bar{A}_2$	
						$-15B - \frac{6}{27}A_4$	$\frac{-2\sqrt{10}}{27}A_4$		$\frac{4\sqrt{10}}{7\times 27}\bar{A}_4 + \frac{24\sqrt{10}}{7\times 15}\bar{A}_2 + \frac{84}{7\times 15}\bar{A}_2$

[a] For explanation of symbols see text.

tet states as long as spin–orbit coupling is small. The ligand field parameters are

$$Dq = \frac{ze^2}{6}R_4$$

and

$$Ds = \frac{2ze^2}{7}R_2$$

where

$$R_4 = \int_0^\infty [R_{3d}(r)]^2 \frac{r_<^4}{r_>^5} r^2\, dr$$

and

$$R_2 = \int_0^\infty [R_{3d}(r)]^2 \frac{r_<^2}{r_>^3} r^2\, dr$$

and the symbols have their usual meanings. Instead of the customary Dt parameter a dimensionless quantity E'/E is employed in our model. This parameter enters through the expressions $\eta = (E + E')/2E$ and $\bar{\eta} = (E - E')/2E$ which modify R_4 and R_2 yielding the parameters $A_4 = ze^2R_4\eta$, $\bar{A}_4 = ze^2 \cdot R_4\bar{\eta}$, and $\bar{A}_2 = ze^2R_2\bar{\eta}$ of Table II. Then $Dq'\eta = {}^1/_6A_4$, $Dq' \cdot \bar{\eta} = {}^1/_6\bar{A}_4$, and $Ds'\bar{\eta} = {}^2/_7\bar{A}_2$. Even though Dq' and Ds' are formally equivalent to Dq and Ds and have physical meanings analogous to those of the usual Dq and Ds parameters, we used primed values since Dq values obtained from fitting spectra correspond to $\eta Dq'$ values of the present model. η and $\bar{\eta}$ provide a measure of the difference in effective charge residing at the antipyrine and halogen ligand sites and, thereby, a measure of covalency effects. The parameters η and $\bar{\eta}$ arise since the development of the weak ligand field Hamiltonian leads to expressions $eR_4[ze + z'e]$ and $eR_2[ze - z'e]$ in terms of the model shown in Figure 3. Parametrization of the effective charges ze and $z'e$ on the two types of ligands would result in four ligand field parameters, rather than three, as in the ionic point-charge approach. An improvement in fit to experiment would not result, since the relevant quantity is the difference between ze and $z'e$, which is described by $(z + z')/2z$ and $(z - z')/2z$, leading to the parameters η and $\bar{\eta}$ in our formulation. For a tetrahedral compound CoA_4 one would have $E = E'$; hence, $\eta = 1$ and $\bar{\eta} = 0$. For compounds of the type CoA_2B_2, $E \neq E'$. In terms of η and $\bar{\eta}$ the specific value of ze is not important and becomes the "dummy parameter" E. In all calculations the dummy parameter E was set equal to 1000 and the quantities η and $\bar{\eta}$ were varied *via* E'. In Figure 3 the halogen ligands are given by $Z'e$.

The fit of the present model to experimental results is demonstrated in Table III. For the dihalogenobis(antipyrine)cobalt(II) complexes the calculated electronic transitions differ from experimental values by no more than the experimental accuracy in determination of band positions. The lowest energy three d ← d bands, for which we did not obtain data because of instrumental limitations, lie at reasonable positions.[13] The conventional model for C_{2v} complexes applied to these complexes did not yield adequate fits to observed spectra—an observation which constituted the initial motivation for undertaking the present formulation.

Table III. Calculated and Experimental Energy Levels for Pseudotetrahedral Bis(antipyrine)cobalt Dihalide Complexes[d]

	$Co(apy)_2I_2$[a]		$Co(apy)_2Br_2$		$Co(apy)_2Cl_2$	
B, cm^{-1}	725		760		770	
Dq', cm^{-1}	−520		−490		−490	
Ds', cm^{-1}	−850		−530		−500	
E'	1900		2200		2300	
Energies, cm^{-1}	Calcd	Exptl[b]	Calcd	Exptl[b]	Calcd	Exptl[b]
	16,401	16,300	16,856	16,800	17,174	17,100
	15,108	15,200	15,786	15,700	16,077	16,200
	14,036	14,000	14,908	14,800	15,185	15,200
	6,733	6,700	7,243	7,200	7,532	7,400
	5,843	5,900	6,068	6,100	6,253	6,250
	5,158	5,100	5,279	5,200	5,427	5,300
	3,738	[c]	3,767	[c]	3,852	[c]
	3,345	[c]	3,484	[c]	3,593	[c]
	2,518	[c]	2,621	[c]	2,675	[c]
	0	0	0	0	0	0

[a] apy = $C_{11}H_{12}ON_2$ (antipyrine). [b] Experimental energy levels could be measured to only about ±100 cm^{-1}. [c] Not observed. [d] The ordering of energy level symmetry labels (C_{2v}) is as shown in Figure 7.

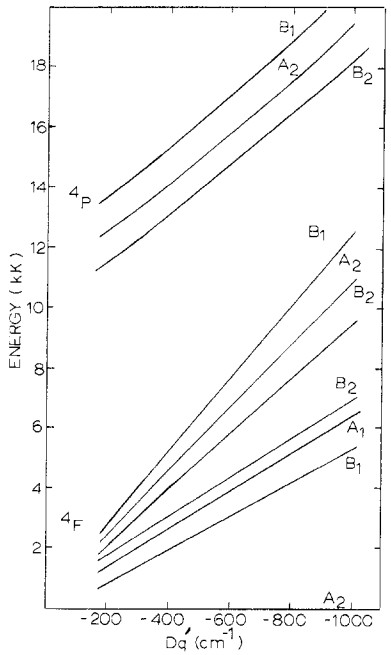

Figure 4. Dependence of energy levels of cobalt(II) complexes with C_{2v} pseudotetrahedral geometry on Dq' ($B = 725$ cm^{-1}, $Ds' = -850$ cm^{-1}, $E' = 1900$).

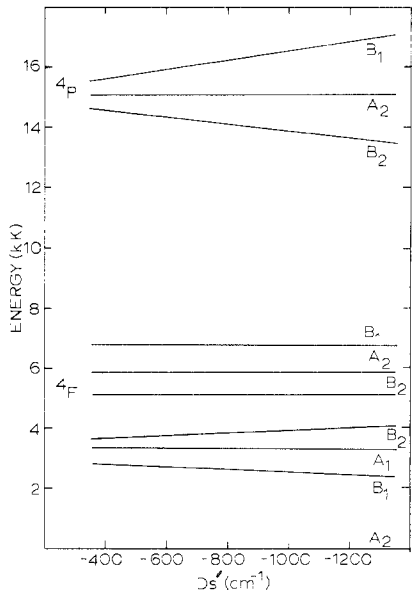

Figure 5. Dependence of energy levels of cobalt(II) complexes with C_{2v} pseudotetrahedral geometry on Ds' ($B = 725$ cm^{-1}, $Dq' = -520$ cm^{-1}, $E' = 1900$).

The dependence of energy levels on ligand field parameters is shown in Figures 4-6. The splitting of the highest orbital triplet for tetrahedral complexes arising from the ^4F term on going to C_{2v} microsymmetry is primarily determined by the parameter E'. The splitting of the ^4P term is dominantly affected by E' and Ds'. The overall splitting of the ^4F term is influenced mostly by E' and Dq'. Finally, the position of the center of gravity of the ^4P term is determined primarily by E' and B. Consideration of parameters in this order together with Figures 4-6 provide a recipe for obtaining reasonably adequate initial trial parameters which can be refined by iterative calculations or by least-squares fitting procedures. For the cobalt(II)-antipyrine complexes least-squares fitting was not necessary since iterative calculations very rapidly yielded fit to within experimental error in the determination of band positions.

To test the general utility of the present model for the electronic spectra of C_{2v} pseudotetrahedral cobalt(II) complexes the data reported in Table V of ref 14 were fitted. In Table V of ref 14 a number of misprints were noted: ref 6 should read ref 7, ref 13 should read ref 16, ref 12 should read ref 15, and the reference for $Co(tu)_2X_2$ complexes should be ref 14. Correspondence of calculated and experimental electronic transition energies is shown in Table IV. Again, least-squares fitting was not necessary. The fits are satisfactory with the exception of the fit to $Co[(C_6H_5)_3P]_2X_2$ (X = Cl, Br, I). From the size of the splitting of the group of lines in the 6000-10,000-cm^{-1} region, arising presumably from the $(^4F)T_1$ parent tetrahedral state, we deduce that the deviation from T_d symmetry is very pronounced. Thus, it is not surprising that the present model, designed for pseudotetrahedral situations, begins to break down. A more serious problem arises from the conflicting reports on the observed band positions for the $Co[(C_6H_5)_3P]_2X_2$ compounds. The reference cited in Table V of ref 14 in connection with these compounds (ref 16) does not correspond to these compounds, which are treated, however, by ref 11 of ref 14. The bands reported in this reference[20] do not correspond to those shown in Table V of ref 14. The crystal spectra reported by Simo and Holt[9] appear to be the most definitive study of the $Co[(C_6H_5)_3P]_2Cl_2$ electronic spectra. The polarizations reported are in apparent conflict with our mod-

Table IV. Calculated and Experimental Energy Levels for Pseudotetrahedral Cobalt Complexes of the Type CoA_2B_2[d]

	$Co(tu)_2I_2$[a]		$Co(tu)_2Br_2$		$Co(tu)_2Cl_2$	
B, cm^{-1}	644		696		719	
Dq', cm^{-1}	−500		−490		−480	
Ds', cm^{-1}	−580		−560		−520	
E'	2200		2300		2450	
Energies, cm^{-1}	Calcd	Exptl[14]	Calcd	Exptl[14]	Calcd	Exptl[14]
	15,399	15,300	16,252	16,200	16,749	16,700
	14,188	14,200	14,996	15,000	15,447	15,500
	13,226	13,300	13,999	14,000	14,425	14,400
	7,319	7,310	7,488	7,570	7,768	7,600
	6,141	6,250	6,227	6,150	6,379	6,170
	5,384	5,300	5,428	5,450	5,541	5,550
	3,815		3,850		3.900	
	3,554		3,592		3,679	
	2,622		2,611		2,625	
	0	0	0	0	0	0
	$Co(EPTCH)_2I_2$[b]		$Co(EPTCH)_2Br_2$		$Co(EPTCH)_2Cl_2$	
B, cm^{-1}	620		666		680	
Dq', cm^{-1}	−465		−480		−500	
Ds', cm^{-1}	−500		−550		−660	
E'	2400		2400		2400	
Energies, cm^{-1}	Calcd	Exptl[14]	Calcd	Exptl[14]	Calcd	Exptl[14]
	15,009	14,970	15,949	15,870	16,647	16,530
	13,781	13,850	14,604	14,590	15,020	15,270
	12,827	12,930	13,559	13,600	13,777	13,700
	7,350	7,400	7,597	7,540	7,888	7,850
	6,059	6,090	6,268	6,370	6,528	6,660
	5,293	5,170	5,466	5,350	5,695	5,550
	3,706		3,849		4.033	
	3,512		3,625		3,773	
	2,520		2,575		2,595	
	0	0	0	0	0	0
	$Co(C_7H_6N_2)_2I_2$[c]		$Co(C_7H_6N_2)_2Br_2$		$Co(C_7H_6N_2)_2Cl_2$	
B, cm^{-1}	680		715		745	
Dq', cm^{-1}	−480		−485		−423	
Ds', cm^{-1}	−350		−250		−200	
E'	2700		2800		3400	
Energies, cm^{-1}	Calcd	Exptl[10]	Calcd	Exptl[10]	Calcd	Exptl[10]
	16,280	16,260	16,727	16,860	17,272	17,240
	15,246	15,240	15,970	15,870	16,471	16,260
	14,438	14,510	15,357	15,380	15,832	15,820
	8,467	8,580	8,880	8,950	9,283	9,260
	6,800	6,670	7,071	6,830	7,160	6,990
	5,912	5,850	6,116	6,060	6,192	6,170
	4,007		4,090		4,122	
	3,944		4,086		3,950	
	2,874		3,074		2,958	
	0	0	0	0	0	0
	$Co[(C_6H_5)_3P]_2I_2$		$Co[(C_6H_5)_3P]_2Br_2$		$Co[(C_6H_5)_3P]_2Cl_2$	
B, cm^{-1}	575		575		586	
Dq', cm^{-1}	−263		−300		−320	
Ds', cm^{-1}	−140		−180		−220	
E'	~5600		~5600		~5600	
	Calcd	Exptl[14]	Calcd	Exptl[14]	Calcd	Exptl[14]
Energies, cm^{-1}	14,802	14,720	15,968	15,750	16,922	16,760
	13,647	14,000	14,416	15,250	14,982	16,000
	12,845	12,880	13,399	13,440	13,775	13,780
	9,149	8,900	10,329	10,000	10,955	10,500
	6,611	7,000	7,462	7,550	7,920	7,840
	5,884	5,700	6,704	6,130	7,133	6,330
	3,835		4,379		4,679	
	3,174		3,564		3,788	
	2,312		2,531		2,581	
	0	0	0	0	0	0

[a] tu = thiourea. [b] EPTCH = $C_6H_5NH(CS)OC_2H_5$. [c] $C_7H_6N_2$ = benzimidazole. [d] The ordering of energy level symmetry labels (C_{2v}) is as shown in Figure 7.

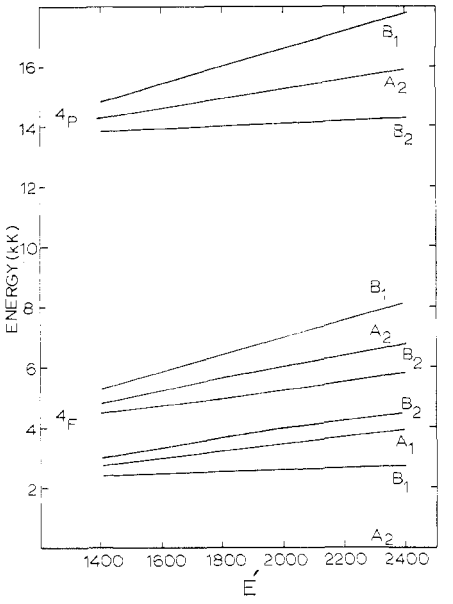

Figure 6. Dependence of energy levels of cobalt(II) complexes with C_{2v} pseudotetrahedral geometry on E' ($B = 725$ cm^{-1}, $Dq' = -520$ cm^{-1}, $Ds' = -850$ cm^{-1}).

el, as well as with the ionic point-charge weak ligand field treatment.[14] We defer discussion of this apparent discrepancy to a later section of this paper. In view of the conflicting reports on band positions[14,20] for $Co[(C_6H_5)_3P]_2X_2$ complexes the data corresponding to these compounds listed in Table IV may not be reliable and need to be disregarded for purposes of judgment of the quality of fit to experiment. Inspection of Table IV shows that the fit to experiment becomes worse, as the deviation from T_d symmetry increases, which is to be expected. Still, the fits to experiment are improved over the previous treatment[14] as we shall show.

The observation of splitting into generally three observed levels of the parent $(^4F)T_1$ and $(^4P)T_1$ tetrahedral bands is indicative of an A_2 ground state. The matrices and associated eigenfunctions of ref 14 lead, however, to an A_1 ground state, which would result in only two electric dipole allowed bands corresponding to a T_1 parent. We therefore checked the symmetry labels for the eigenvectors in Table II of ref 14. Reflections through the xz and yz planes lead to $(2,1,-1) \rightarrow (-2,-1,1)$ and $(1,-1,-2) \rightarrow (-1,1,2)$. However, $(-2,-1,1)$ cannot be directly equated to $(1,-1,-2)$. A permutation must be performed: $(-2,-1,1) = -(1,-1,-2)$. One obtains, for instance, that the state $(1/i)\sqrt{1/2}[(2,1,-1) - (1,-1,-2)]$ is invariant under the C_{2v} group operations and, hence, is A_1. A similar situation holds for the other C_{2v} states. The C_{2v} symmetry label subscripts 1 and 2 of Table II of ref 14 need therefore to be interchanged. With this correction the ordering of states in terms of their associated symmetries becomes the same as that of our formulation. We have employed the matrices and parameters of Table IV of ref 14 and have calculated energy levels by computer. The results do not agree with those shown in Figure 1 of ref 14. Parameters of Table IVA correspond to C_{2v} spectrum C rather than A in Figure 1 of ref 14, excepting the lowest level in energy. We found 17.15, 15.98, and 15.48 kK. The parameters of Table IVC give best agreement with the C_{2v} spectrum A rather than C of ref 14, again with the exception of the lowest level. We obtain 16.28, 15.07, and 14.45 kK. For the parameters of Table IVB of ref 14 we obtain 16.96, 15.32, and 14.58 kK. Here, too, the lowest level differs from Figure 1B of ref 14. Several elements of the C_{2v} matrices of ref 14 were checked. The appropriate degeneracies result when the parameters Ds and Dt are set to zero. Fits to the spectrum of $Co(tu)_2Br_2$ (tu = thiourea) by use of both our formulation and that of ref 14 were performed. The comparison is shown in Figure 7. The fit with our formulation is better; symmetry labels of both treatments agree. We note that the development of our model uses x and y axes rotated about z by 45° with respect to those appropriate to the formulation of ref 14 (see Figure 3). Instead of $y \rightarrow -y$ and $x \rightarrow -x$ as a result of the C_{2v} operations $\sigma_v(xz)$ and $\sigma'_v(yz)$, respectively, we have $y \rightarrow -x$, $x \rightarrow -y$ and $y \rightarrow x$, $x \rightarrow y$ resulting from the operations σ_v and σ'_v. The symmetries of eigenvectors in our formulation are not as conveniently obtained as in the formulation shown in ref 14 but can be obtained by performing the C_{2v} symmetry operations on the computer-obtained eigenvectors, which are linear combinations of the basis states of Table II. Table VA shows the expected linear combinations. The letters in Table VA represent the numerical coefficients corresponding to the basis functions (in the same order) of Table II. Table VB shows eigenvectors obtained by computer. If one allows for small numerical discrepancies, which must be expected because of truncations introduced by the computer during the performance of numerical evaluations (we did not use double precision), then the correspondence of Table VB to Table VA emerges.

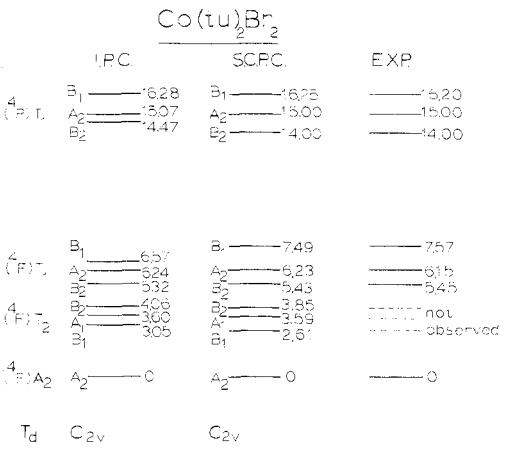

Figure 7. Comparison of fits to experiment[14] (EXP.) employing the ionic point-charge (I.P.C.) weak ligand field treatment[14] ($B = 700$ cm^{-1}, $Dq = -310$ cm^{-1}, $Dt = 120$ cm^{-1}, $Ds = 720$ cm^{-1}) and our semicovalent point-charge (S.C.P.C.) weak ligand field formulation (using the parameters of Table IV). Energies are given in kK.

Unfortunately, observed spectra are not always sufficiently well resolved to readily allow determination of band positions of a given orbital parent triplet just by inspection. A case which falls into this category is $Co(apy)_2(NCS)_2$. Spectral data for this complex will be reported elsewhere.[15] Inspection of the spectrum allowed only rough estimates of band positions for the highest lying ^4F orbital triplet. For the ^4P term only two band positions could be estimated. Assuming gaussian band shapes it was possible to fit the observed bands with the required three bands by gaussian analysis[16] on a computer. Figures 8 and 9 show calculated and observed spectra as well as the component gaussian bands. Calculated component band positions agree with estimates made by inspection of the raw data. Thus, gaussian spectral fitting provides an additional convenient tool which extends

(20) F. A. Cotton, O. D. Faut, D. M. L. Goodgame, and R. H. Holm, *J. Amer. Chem. Soc.*, 83, 1780 (1961).

Table V. Predicted (A) Coefficients of the Respective Basis States (Table II) for Eigenfunctions of C_{2v} Symmetry and Computer-Generated (B) Coefficients ($B = 700$ cm^{-1}, $Dq' = -620$ cm^{-1}, $Ds' = -100$ cm^{-1}, $E' = 1200$) with Analogous Order Based on the Matrix of Table II[a]

T_d	C_{2v}	Coefficients									
						A					
$(^4P)T_1$	B_1	a_1		b_1		b_1		a_1	c_1		c_1
	A_2				a_2					b_2	
	B_2	a_3		$-b_3$		b_3		$-a_3$	$-c_3$		c_3
$(^4F)T_1$	B_1	a_4		b_4		b_4		a_4	c_4		c_4
	A_2				a_5					b_5	
	B_2	a_6		$-b_6$		b_6		$-a_6$	$-c_6$		c_6
$(^4F)T_2$	B_2	a_7		$-b_7$		b_7		$-a_7$	$-c_7$		c_7
	A_1		a_8				a_8				
	B_1	a_9		b_9		b_9		a_9	c_9		c_9
	A_2		$-a_{10}$				a_{10}				
						B					
$(^4P)T_1$	B_1	0.0798	0	0.0544	0	0.0544	0	0.0798	0.7005	0	0.7005
	A_2	0	−0.0059	0	−0.1358	0	−0.0066	0	0	0.9907	0
	B_2	−0.0718	0	0.0632	0	−0.0632	0	0.0718	0.7006	0	−0.7006
$(^4F)T_1$	B_1	0.5309	0	0.4572	0	0.4572	0	0.5308	−0.0959	0	−0.0959
	A_2	0	−0.0110	0	0.9907	0	0.0024	0	0	0.1357	0
	B_2	−0.5824	0	0.3897	0	−0.3897	0	0.5824	−0.0948	0	0.0948
$(^4F)T_2$	B_2	−0.3946	0	−0.5866	0	0.5866	0	0.3946	0.0125	0	−0.0125
	A_1	0	0.7070	0	0.0048	0	0.7071	0	0	0.0096	0
	B_1	−0.4603	0	0.5367	0	0.5367	0	−0.4602	0.0108	0	0.0108
	A_2	0	−0.7071	0	−0.0095	0	0.7071	0	0	−0.0008	0

[a] See text for discussion.

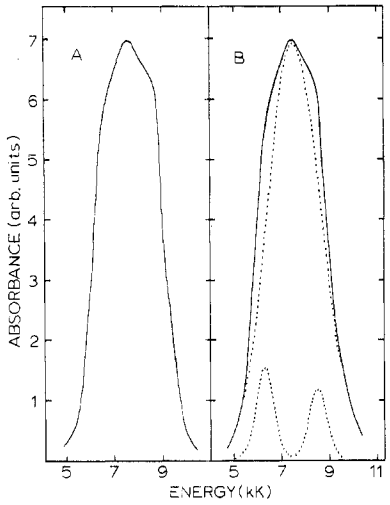

Figure 8. Near-infrared absorption spectra of $Co(apy)_2(NCS)_2$ in dichloromethane: (A) observed spectrum; (B) calculated spectrum (–) and component gaussian bands (· · ·).

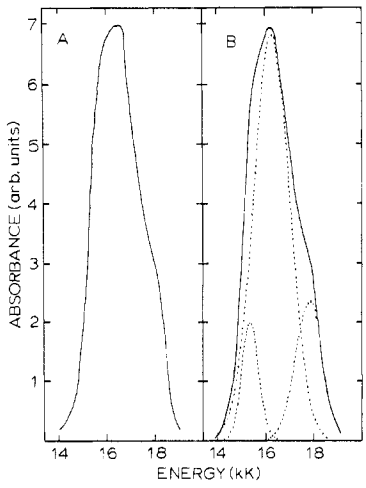

Figure 9. Visible spectra of $Co(apy)_2(NCS)_2$: (A) observed spectrum; (B) calculated spectrum (–) and component gaussian bands (· · ·).

the applicability of the present ligand field model to spectra which do not exhibit well-resolved bands. The ligand field fit for $Co(apy)_2(NCS)_2$ is given in Table VI. For reasonably well-resolved spectra gaussian analysis yields accurate band positions, widths, and intensities. These are useful for calculation of radiative rates which are of interest if radiationless molecular relaxation processes are to be studied.

Discussion

Addition of spin–orbit coupling effects can be made adequately only for spectra exhibiting sharper structure than that obtained for the $Co(apy)_2X_2$ complexes. Moreover, the positions of the spin-doublet terms need be known, particularly those near the ^4P term. However, their spin-forbidden nature generally precludes experimental observation. Under these circumstances consideration of spin–orbit coupling was not feasible in the present study. In any event the excellence of obtained fit of the model to experiment suggests that spin-orbit coupling does not play a significant role in the determination of the structure of the spectra of the complexes studied.

The spectra of the antipyrine complexes exhibit the anticipated behavior with regard to the spectrochemical series for halide ligands.[21] The trend in nephelauxetic effects also follows expectations. We denote the halide ligands by left superscripts on ligand field parameters and consider their magnitudes as a function of the halogen. Correlation with the usual Dq parameter is obtained by inspection of $Dq'\eta$ of the present model. The sequence $|^{Cl}Dq'\eta| > |^{Br}Dq'\eta| > |^{I}Dq'\eta|$ is as anticipated. In terms of increasing covalency in the order Cl < Br < I the chloride ion can be expected to differ most from the effective charge of the antipyrine ligand which binds the metal ion *via* the carbonyl oxygen atom. The sequence $^{I}\eta < ^{Br}\eta < ^{Cl}\eta$ is also reasonable.

The complex interplay between electrostatic and covalency effects in the determination of trends in magnitude of the ligand field parameter Dq and the Ds/Dq ratio in relation to the spectrochemical series has been discussed by Gerloch and Slade.[22] They show (ref 22, Table 7.1) that (1) with

(21) Reference 18, pp 76–84.
(22) M. Gerloch and R. C. Slade, "Ligand Field Parameters," Cambridge University Press, Cambridge, 1973, pp 140–145.

Table VI. Calculated and Experimental Energy Levels (cm^{-1}) for $Co(apy)_2(NCS)_2$[d]

Calcd[a]	Exptl[b]	Exptl[c]
17,987	17,880	18,000
16,392	16,340	16,300
15,137	15,390	
8,575	8,590	8,500
7,245	7,460	7,400
6,374	6,360	6,300
4,535		
4,196		
3,053		

[a] Parameters are $B = 735$ cm^{-1}, $Dq' = -600$ cm^{-1}, $Ds' = -790$ cm^{-1}, and $E' = 2150$. [b] Obtained by fitting observed spectra to gaussian bands. For details see text. [c] Obtained by inspection of raw data to within about ±100 cm^{-1}. [d] The ordering of energy level symmetry labels (C_{2v}) is as shown in Figure 7.

Table VII. Parameters for Cobalt(II)-Antipyrine Complexes

Parameters	Co-$(apy)_2$-I_2[b]	Co-$(apy)_2$-Br_2	Co-$(apy)_2$-Cl_2	Dominant Mechanism[c]
η[a]	1.45	1.6	1.65	
$-Dq'$	520	490	490	Covalent
$-Ds'$	850	530	500	
$-\eta Dq'$[a]	754	784	808	
Ds'/Dq'	1.63	1.08	1.02	Electrostatic

[a] The correlation with the spectrochemical series is described by the parameters η and $-\eta Dq'$ (rather than Dq) in the present model. See text for definition of η. [b] apy = antipyrine. [c] For discussion see text.

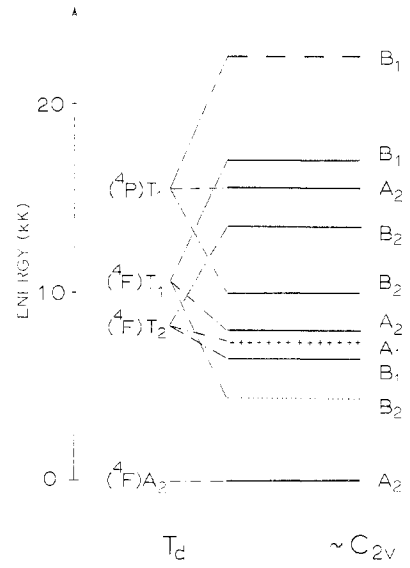

Figure 10. Scheme to reconcile experimental symmetry assignments[9] with weak ligand field theoretical assignments (see Figure 7) for $Co[(C_6H_5)_3P]_2Cl_2$. See text for justification of this scheme and discussion of levels.

increased metal-ligand bond length, Dq decreases and the Ds/Dq ratio increases, (2) with transfer of negative charge to the metal, Dq increases and Ds/Dq decreases, and (3) transfer of negative charge from the ligand results in Dq decrease while Ds/Dq remains unchanged. The third factor is explicity taken into account by the quantities η and $\bar{\eta}$ of our model. Trends of Dq' and Ds'/Dq' for $Co(apy)_2(halide)_2$ complexes (Table VII) indicate that Dq' is dominated by covalency effects (factor 2 above) whereas Ds'/Dq' is influenced primarily by electrostatic, *i.e.*, bond length, effects.

The primary weakness of the ionic point-charge as well as the present semicovalent weak ligand field treatments concerns their apparent conflict with the symmetry assignments[9] in the study of $Co[(C_6H_5)_3P]_2Cl_2$. This discrepancy was noted in the work of Tomlinson, Bellitto, Piovesana, and Furlani.[23] The symmetry labels in their Figure 5(b) are not the same as those of Flamini, Sestili, and Furlani.[14] Apparently, the previously mentioned correction in terms of permutations on wave functions as well as a change in x and y axes was performed. Still, the resulting order of states, analogous to that of our formulation, does not agree with the results of Simo and Holt.[9] A flipping of the order of the $(^4P)T_1$ states was achieved by use of purely empirical low-symmetry parameters.[23] These are difficult to justify[23] and do not produce adequate correspondence between calculated and observed energy level positions.[23] The evidently unsatisfactory correspondence of theory (our model, as well as those of Furlani, *et al.*)[23] with experiment brings to mind the possibility that the tetrahedral parent assignments associating the levels at about 17,000, 15,750, and 13,550 cm^{-1} with $(^4P)T_1$ and 10,700, 8000, and 6400 cm^{-1} with $(^4F)T_1$ may not be correct, even though the A_2 and $B_{1,2}$ assignments cannot be argued (a misprint occurs in Table I of ref 9—the band at 8000 cm^{-1} should be A_2 rather than B_2). As Simo and Holt pointed out,[9] pseudotetrahedral cobalt(II) complexes (of the C_{2v} type) normally show $(^4F)A_2 \rightarrow (^4F)T_1$ transitions in the 4000–7000-cm^{-1} region and $(^4F)A_2 \rightarrow (^4P)T_1$ transitions in the 15,000–20,000-cm^{-1} region with band widths of the order of some 3000 cm^{-1}. In $Co[(C_6H_5)_3P]_2Cl_2$ the typical $(^4F)T_1$-$(^4P)T_1$ gap is absent. Moreover, one usually finds a strong-charge-transfer absorption near the $(^4P)T_1$ band and just to the blue side of it, which in $Co[(C_6H_5)_3P]_2Cl_2$ has apparently been pushed well to the ultraviolet region. These considerations indicate that the deviation from T_d symmetry is very pronounced, which is corroborated by crystal structure study.[24] Thus, the splittings of the $(^4F)T_2$, $(^4F)T_1$, and $(^4P)T_1$ bands may well be so large that overlap results, making assignment of a T_d parent state to an observed C_{2v} level A_2, $B_{1,2}$ difficult. Under these circumstances the pseudotetrahedral models cannot be expected to be applicable in a quantitative sense. We nevertheless attempt an assignment retaining the ordering of A_2 and $B_{1,2}$ states corresponding to the parent T_d manifolds as shown in Figure 7, but the splittings are now allowed to increase vastly. From Tables III, IV, and VI it is seen that in the compounds listed the $(^4P)T_1$ manifold splits typically by about 2000 cm^{-1}, $(^4F)T_1$ by about 2000 cm^{-1}, and $(^4F)T_2$ by about 1200 cm^{-1}. If we maintain these relative sizes of splittings but increase each by roughly a factor 6, we obtain a scheme as shown in Figure 10. Here solid lines correspond to observed levels and symmetries.[9] The A_1 level (++++) is electric dipole forbidden, the lowest level, B_2 (· · · ·), would lie too low to be observed, the highest level, B_1 (– – –), would lie in the 20,000–25,000-cm^{-1} region. Curiously, two weak bands of the right polarization are observed in this region.[9] The scheme in Figure 10 reconciles the theoretically predicted ordering of sublevels of the $T_{1,2}$ parent bands with experiment.[9,23] Relative splittings of the T_d bands are consistent with those of the more nearly tetrahedral CoA_2B_2 complexes. The "theoretically predicted" B_1 band in the 20,000–25,000-cm^{-1} region is consistent with experiment. The need for strong deviation from T_d

(23) A. A. G. Tomlinson, C. Bellitto, O. Piovesana, and C. Furlani, *J. Chem. Soc., Dalton Trans.*, 350 (1972).

(24) G. Garton, D. E. Henn, H. M. Powell, and L. M. Venanzi, *J. Chem. Soc.*, 3625 (1963).

symmetry to allow proposing of the scheme of Figure 10 is consistent with crystal structure results[24] (which indicate that the deviation from T_d in $Ni[(C_6H_5)_3P]Cl_2$, which is isomorphous to $Co[(C_6H_5)_3P]_2Cl_2$, is very pronounced) and with the absence of an observed strong charge-transfer band just to the blue side of about 17,000 cm^{-1}. This reconciliation as well as the good correspondence of our formulation with experiment as seen from Tables IV, VI, and VII lend credibility to the underlying model.

Inspection of Figures 1 and 2 of ref 14 and comparison with our Tables IV, VI, and VII indicate that the present model provides an improvement over previous work. Gaussian fitting of poorly resolved spectra adds to the utility of the model. Where distortion in terms of bond angles and lengths from tetrahedral symmetry is pronounced, a choice between the constant charge-variable ligand distance approach[14] and our variable charge-tetrahedral geometry method might be necessary since the former model may be more physically meaningful. Crystallographic studies, whenever available, should aid this choice. To some extent, geometric distortions are also taken into account by the empirical nature of the parameter Ds' in the present model. The structure of $Co(apy)_2Cl_2$ can be inferred from the data for the isostructural[25] compound $Zn(apy)_2Cl_2$. The crystallographic results show that neither model has much correspondence to the solid-state structure. However, the situation with respect to the solution species may be somewhat better. For the $Co(apy)_2Cl_2$ complexes, therefore, there is little difference in physical significance between the two approaches with regard to molecular geometry assumed. However, if the remarkably good fit to experimental data obtained with the present model is interpreted as attesting to the validity of the assumptions underlying the model, namely, the dominant role of the relative effective charges residing at the sites of the two types of ligands in a given complex over relative bond lengths and angles, then the effective ligand charges play an even more significant role in determining spectral structure than has been heretofore appreciated. Such a role is at least partly accounted for more explicitly in the present approach than in previous weak-field methods. Undoubtedly, a combination of variation in ligand charges and positions represents a still better treatment. Unfortunately, the increased number of required parameters renders such a method impractical in view of the sparsity of observed electronic transitions.

(25) M. B. Cingi, C. Guastini, A. Musatti, and M. Nardelli, *Acta Crystallogr., Sect. B*, 28, 667 (1972).

Acknowledgment. The authors are grateful to Professor R. G. Cavell, University of Alberta, Edmonton, Alberta, Canada, for the Fortran listing of the program BIGAUSS.

Registry No. $Co(apy)_2Cl_2$, 19747-33-2; $Co(apy)_2Br_2$, 19747-34-3; $Co(apy)_2I_2$, 19747-35-4; $Co(apy)_2(NCS)_2$, 20002-46-4.

Contribution from the Department of Chemistry, University of Western Ontario, London, Ontario, Canada

Cobalt(III) Complexes Containing Optically Active Tartaric Acid

ROLAND A. HAINES,* EDWARD B. KIPP, and MONICA REIMER

Received July 13, 1973 AIC30528B

Three monomeric species of the type $[Co(en)_2tart]$, where en is ethylenediamine and tart is an anion of D- or L-tartaric acid, have been isolated. Two of the species are ionic and involve different types of coordination of a dinegative tartrate ion in a chelate ring. The third species is neutral and contains a trinegative tartrate ion. The compounds have been characterized using circular dichroism and electronic and infrared absorption spectra as well as proton nmr spectra.

Introduction

Recently it has been shown[1,2] that coordinated hydroxy acid anions can induce very pronounced effects on the observed circular dichroism spectra of certain cobalt(III) complexes. In an extension of these studies we have now prepared certain monomeric complexes containing an optically active tartrate anion. The interest in these complexes arose from the fact that the coordinated ligand had a side chain with additional functional groups which could be influential in the stereochemistry of the product obtained.

Several years ago the preparation of a monomeric species with the general formula $[Co(en)_2tart]Br$ was reported.[3] However the species was shown to be a mixture of two diastereoisomers and no good separation was obtained. More recently some further results have been reported[4] on the preparation of a monomeric species in solution but again a mixture of diastereoisomers was present. Later workers, however, were successful in isolating and characterizing a dimeric species containing a bridging tartrate ion.[5] We have now isolated three monomeric species with the general formula $[Co(en)_2tart]^{n+}$ and report our findings in this paper.

Experimental Section

Reaction of Equimolar Quantities of Carbonatobis(ethylenediamine)cobalt(III) Chloride and Tartaric Acid. A mixture of 1.0 g of $[Co(en)_2CO_3]Cl$, 0.5 g of optically active tartaric acid, and 10–15 ml of water was refluxed on a steam bath for 4 hr. The mixture was then transferred to an evaporating dish and evaporated to dryness on the steam bath. The reddish solid obtained was ground with absolute ethanol, filtered, washed with ether, and dried under a heat lamp; yield 1.2 g.

A concentrated aqueous solution of the above product was spotted on 1-mm tlc plates of Camag DS-O silica gel and developed with water. Three bands separated, the last of which was pink and was only a minor component of the mixture. Bands 1 and 2 (red and purple,

(1) E. B. Kipp and R. A. Haines, *Inorg. Chem.*, 11, 271 (1972).
(2) R. A. Haines and A. A. Smith, *Inorg. Chem.*, 12, 1426 (1973).
(3) H. B. Jonassen, J. C. Bailar, and E. H. Huffman, *J. Amer. Chem. Soc.*, 70, 756 (1948).
(4) J. H. Dunlop, R. D. Gillard, and N. C. Payne, *J. Chem. Soc. A*, 1469 (1967).
(5) R. D. Gillard and M. G. Price, *J. Chem. Soc. A*, 1813 (1969).